



**HAL**  
open science

## Partial Discharge Measurements on Glass-Mica-Epoxy Samples for electrical insulation during Accelerated Thermo-Oxidative Aging

Pierre Schlupp, Vincent Boucher, Pascal Rain, André Petit

► **To cite this version:**

Pierre Schlupp, Vincent Boucher, Pascal Rain, André Petit. Partial Discharge Measurements on Glass-Mica-Epoxy Samples for electrical insulation during Accelerated Thermo-Oxidative Aging. IN-SUCON: International Electrical Insulation Conference, May 2009, Birmingham, United Kingdom. pp163-170. hal-00391264

**HAL Id: hal-00391264**

**<https://hal.science/hal-00391264>**

Submitted on 3 Jun 2009

**HAL** is a multi-disciplinary open access archive for the deposit and dissemination of scientific research documents, whether they are published or not. The documents may come from teaching and research institutions in France or abroad, or from public or private research centers.

L'archive ouverte pluridisciplinaire **HAL**, est destinée au dépôt et à la diffusion de documents scientifiques de niveau recherche, publiés ou non, émanant des établissements d'enseignement et de recherche français ou étrangers, des laboratoires publics ou privés.

# PARTIAL DISCHARGE MEASUREMENTS ON GLASS-MICA-EPOXY SAMPLES FOR ELECTRICAL INSULATION DURING ACCELERATED THERMO-OXIDATIVE AGING.

P. Schlupp<sup>1</sup>, V. Boucher<sup>1,2</sup>, P. Rain<sup>2</sup>, A. Petit<sup>3</sup>

<sup>1</sup> Electricité de France (EDF) – R&D, France

<sup>2</sup> Grenoble Electrical Engineering lab (G2Elab), CNRS - Université de Grenoble, France

<sup>3</sup> Electricité de France (EDF) – DTG, France

## ABSTRACT

The stator windings of large air-cooled rotating machines are mainly insulated with mica-glass fabric impregnated with epoxy resin. In service, these materials are submitted to thermal, mechanical and electrical stresses. A specific aging arrangement has been set-up allowing artificial thermo-oxidative aging of samples, thanks to the application of a dry O<sub>2</sub> pressure at a controlled temperature. Three different materials, one reference material and two candidate materials, of different thermal classes or different thermal conductivity, have been aged and compared. Partial Discharges (PD) analysis of the samples has been conducted and correlated with samples' morphology. Because of the small size of the samples, a specific PD measurement arrangement has also been set-up. After only a few hundred hours aging, delaminations of a few tens of μm were observed within the samples. PD measurements revealed a decrease of the PD Inception Voltage (PDIV) on these aged samples. The PDIV on samples with specific cavity thickness were also in good agreement with Paschen law. PD measurements, especially the PDIV, seem to be a good indicator of the progress of the aging.

## INTRODUCTION

Mica-glass fabric impregnated with epoxy resin is commonly used as insulator in 20 kV rotating machines. Once the voltage is rated, the power generated by the rotating machine is limited by the temperature that the machine is able to withstand without damaging its insulation. In order to increase the power provided by the generator, two ways are commonly used: increasing the maximum temperature withstand by the insulation (its thermal class temperature, in accordance with IEC 60216 and IEC 60085), or increasing its thermal conductivity to improve the evacuation of heat. These two solutions will be considered and compared hereafter with two specific materials.

Since the mechanical stress is not taken into account in this work, and since the sheets of mica provide a good protection against the propagation of possible electrical trees, temperature-enhanced oxidation is considered here as the main aging factor of these insulating systems, at least in the first steps of aging. Oxygen

pressure has shown itself relevant to accelerate thermo-oxidative aging [1,2]. Then, samples of the two materials are submitted to highly thermo-oxidative aging, in order to accelerate their degradation. The samples have been followed in mass, Dynamic Mechanical Analysis (DMA) and dielectric spectroscopy [3,4]. The purpose here is to investigate their behaviour in terms of Partial Discharges (PD) and morphology.

## EXPERIMENTAL PART

### Materials

Materials are composites of mica paper and epoxy resin reinforced by glass fibre. A ribbon of glass fabric covered with mica paper is wrapped around the copper bar of the generator. Then the bars are impregnated and cured following a VPI process. Cross-linking is generally incomplete, and is achieved during the first uses of the generator.

Three different materials, one reference material and two candidate materials are considered in this study; both candidate materials are still prototypes. First one is a High Conductivity Tape material, which is a class 155 (F) insulation, filled with Boron Nitride powder, which increases significantly the thermal conductivity of the material, so called "HC-F". In the second one, the epoxy resin is formulated to fulfil thermal class 180 (H), so called "Class-H". The reference material is also a class 155 (F) insulation, so called "Ref-F".

### Sampling

Insulation plates are cut and pulled up from their copper bars, then sanded down to smooth their surfaces and remove the conductive coating. Samples are then cut using a diamond saw. Two types of sample shapes have been used: rectangular samples (85x10x5 mm<sup>3</sup>) and square samples (60x60x5 mm<sup>3</sup>).

Diamond saw is cooled by water; samples are then dried during one week at 50°C to remove a large part of the water. Drying ends during post-curing.

As the epoxy cross-linking is not completed during the manufacturing process, samples are post-cured. Curing temperature is chosen above glass transition temperature (120°C for the class 155 materials, 155°C

for class 180 material). Efficiency of drying and curing are respectively checked by following the evolution of mass and the evolution of glass transition temperature.

### Aging arrangement

A test arrangement has been designed to submit samples to both thermal and oxidative stresses (Figures 1, 2 and 3). Samples were laid in glass plates, which were set inside a stainless steel rack standing in each pressure chamber (a to d). Two similar ovens (1 and 2) contain each two chambers connected to the gas tank. The two chambers of a same oven can be isolated thanks to a gate. A vacuum pumping is applied before filling the vessel with oxygen. The gas is supplied by Air Liquide with less than 3 ppm of gaseous impurities and water. This device allows an aging temperature up to 200°C and a pressure up to 10 bars.

All three materials have been compared during aging at their thermal class temperature, under oxygen pressure (2.3 bars) or under air at atmospheric pressure. For more details on the aging procedures see reference [3].

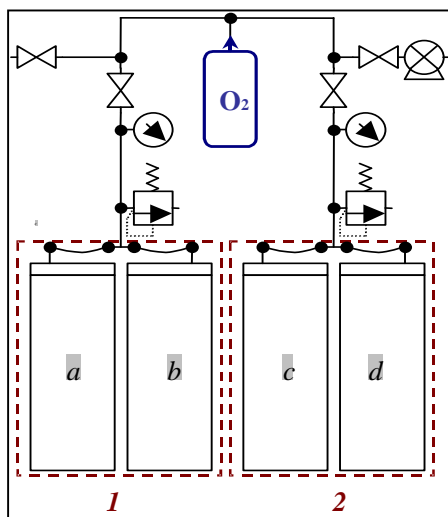


Figure 1: Aging arrangement



Figure 2: Oven 1 with pressure chambers a and b



Figure 3: Stainless steel rack with glass plates and samples

### Aging characterisation

In order to characterize the aging of the materials, different measurement techniques have been tried. The most sensitive techniques to evaluate the aging of the samples have proven to be:

- Mass loss measurements,
- Dynamic Mechanical Analysis, in order to measure Glass Transition temperature ( $T_g$ ) and Young modulus,
- Dielectric Spectroscopy Analysis, and
- Partial Discharge (PD) measurements.

The main results of the Mass loss measurements, Dynamic Mechanical Analysis and Dielectric Spectroscopy Analysis have already been presented in [3] and [4]. So here only the PD measurement arrangement and results will be presented and discussed.

### Partial Discharge measurement arrangement

The aging of an insulation system may lead to the formation of voids, cracks or delaminations inside the material or the increase of their sizes. The appearance of PDs is then a natural consequence of those cavities. To a certain extent, the Partial Discharge Inception Voltage (PDIV) and the PD patterns (number and magnitude of PDs versus test voltage phase) may be associated to the type of defect and the geometry and size of the voids [5-6].

Due to the samples small size and rigidity, a specific PD measurement arrangement had to be developed (figure 4). The sample is clenched between two brass electrodes. In order to avoid surface discharges, the samples, as well as the electrodes, are immersed in a cell filled with a dielectric liquid. The cell itself is made of PTFE (Teflon) and watertight, except openings at the top for the liquid filling up and degassing under vacuum.

The samples are square,  $60 \times 60 \text{ mm}^2$ . To minimize the risk of flashover issued from creeping discharges, the electrodes have a diameter of 35 mm (figure 5).

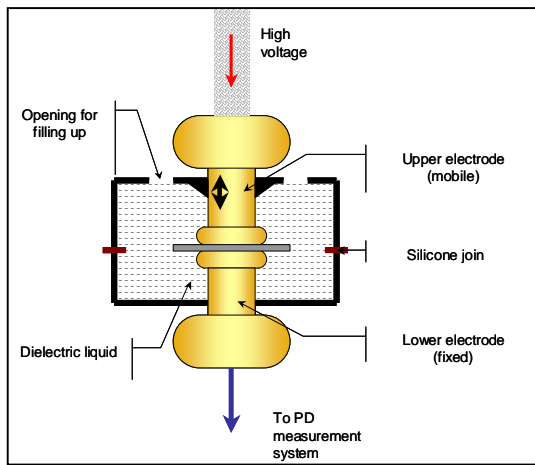


Figure 4: PD measurement cell

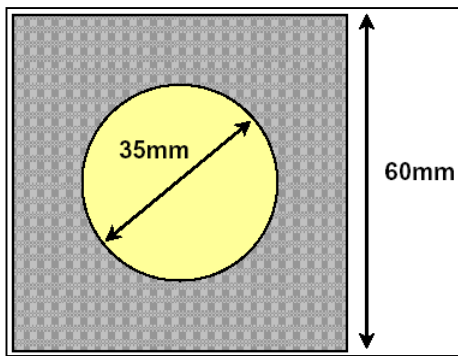


Figure 5: Sample and electrode sizes

In order to minimize interferences, several electronic devices have been used (figure 6): a voltage generator associated to a power amplifier instead of an autotransformer directly connected to the grid, an adjustable resistance, a filter and a capacitive divider. Furthermore, the high voltage part of the circuit is located in a Faraday cage.

The PD measurer is an ICM system from Power Diagnostix. For each voltage level, the recording duration is 100 s. Between each voltage level the recording is stopped for 20 s in order to adjust the next voltage level. The “dead time” after each PD is adjusted to 15  $\mu\text{s}$ . The apparatus is calibrated with a calibrator of 10 pC. In order to reject the background noise, the lower detection limit is adjusted to 2% of the maximum scale. In order to avoid damages to the PD electronics in the case of sample breakdown, a current loop detector is placed between the sample and the PD preamplifier. The purpose is to cut off the generator if a breakdown current is detected.

As the aged samples presented many cracks at the edges (see figure 7, 10 and 11) the dielectric liquid

could penetrate the samples and inhibit the DPs. This is the reason why a silicone gel has been used instead of a dielectric liquid or gas. Afterwards, for more security, the edges of the samples have been varnished. Once the edges are varnished, and since the cleaning of the cell filled with silicone gel revealed tedious, the silicone gel has been abandoned in favour of a vegetable oil. Great care has to be taken in the filling and the degassing of the cell to avoid and eliminate the bubbles. Indeed, these bubbles may be sources of parasitic DPs.

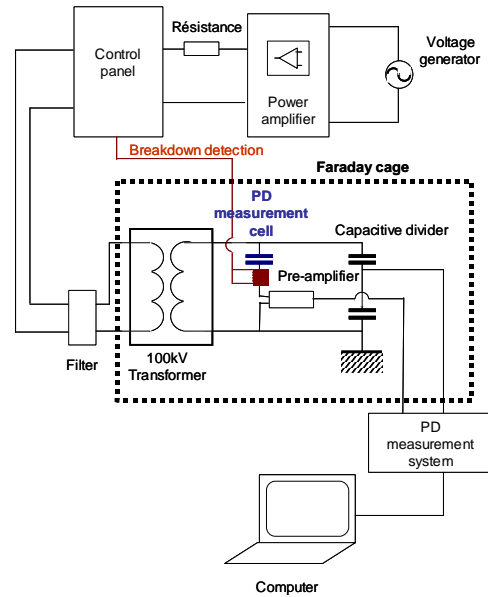


Figure 6: PD measurement electrical circuit diagram

The validation of the PD measurement arrangement has been achieved in two stages. In a first stage, only a reference capacity of 100 pF able to withstand up to 100  $\text{kV}_{\text{rms}}$  has been used. With this reference capacity, the background noise remained low (about 0.3 pC) up to 20  $\text{kV}_{\text{rms}}$ . In a second stage, the reference capacity has been replaced by a Plexiglas sample with varnished edges and having the same size as the real samples. No PD has been measured below 18  $\text{kV}_{\text{rms}}$ . The PD measurement arrangement, cell and electrical circuit, is thus validated up to 18  $\text{kV}_{\text{rms}}$ , with a background noise of about 0.3 pC.

## RESULTS

### PDIV measurements

The PD measurements have been first carried out with a HC-F sample. This sample has been aged during 4250 h, at 155°C and under a  $\text{O}_2$  pressure of 2.3 bar. To make the measurement of the PDs easier, the thickness of the sample has been reduced from 5 mm to 2 mm. As the first measured PDIV was rather low, about 3.8  $\text{kV}_{\text{rms}}$ , the following PDIV measurements have been made with samples with their full thickness (5 mm). The table 1 summarizes the results for different non-aged and aged samples

Sample (aging time)	PDIV ( $kV_{rms}$ )
Ref-F (805 h)	8
HC-F (new)	14
HC-F (4250 h) 2 mm thick	3.8
Class-H (new)	10.7
Class-H (740 h)	8

Table 1: PDIV measurements

## PD patterns

Only few PD pattern have been made at PDIV and above PDIV. The most interesting patterns are presented in figure 7, figure 8 and figure 9.

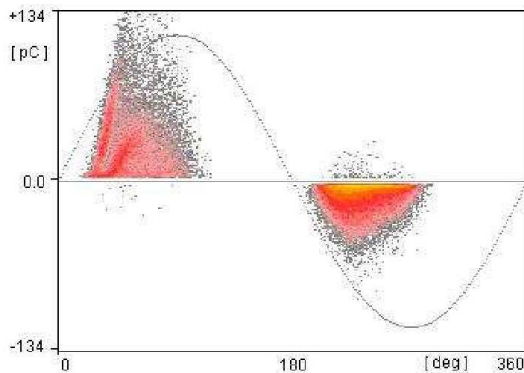


Figure 7: PD pattern at 8 kV (PIDV) for a new Ref-F sample

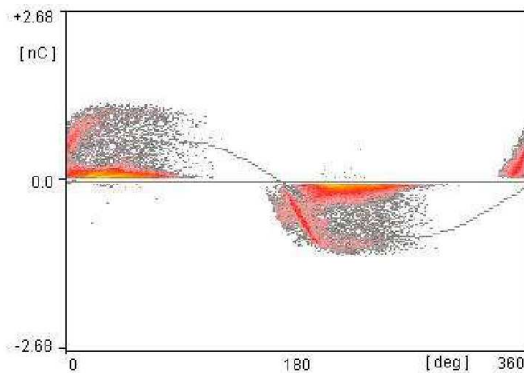


Figure 8: PD pattern at 15 kV for an aged Ref-F sample (805 h, 155°C, 2.3 bar O<sub>2</sub>)

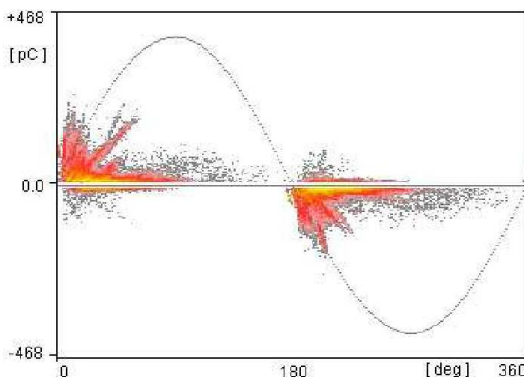


Figure 9: PD pattern at 4.6 kV (PIDV) for an aged HC-F sample (4250 h, 155°C, 2.3 bar O<sub>2</sub>)

## Visual inspection of the samples

To better understand the PDIVs and PD patterns, the presence of voids or delaminations at the edges and also inside the samples has been checked. The samples have been cut as shown in figure 10. The remaining part of the sample, less than 1 mm thick, is then translucent. To check the presence of voids, the surfaces of the remaining parts have been scanned, directly or by back lighting.

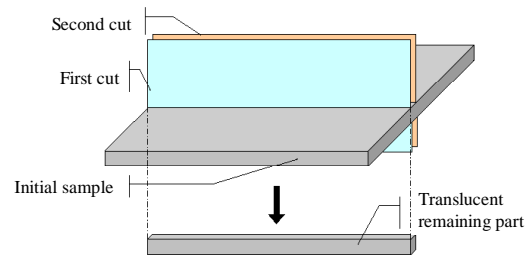


Figure 10: Cutting out of a sample

For the aged Ref-F sample, a single large delamination can be seen inside the sample (figure 11). But it is impossible to know if this delamination has been created during the cutting or if it is the result of the propagation of an existing crack. In any case, it is probably the result of an initial defect. It is also interesting to note that only one delamination of 60  $\mu\text{m}$  thick is present at the edge of the sample (zoom in figure 12), but this delamination goes deep inside the sample.



Figure 11: Scan of an aged Ref-F sample (805 h, 155°C, 2.3 bar O<sub>2</sub>)

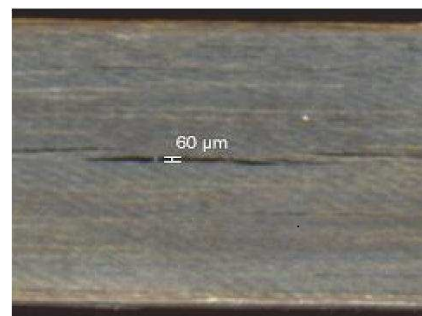


Figure 12: Zoom of the aged Ref-F sample (805 h, 155°C, 2.3 bar O<sub>2</sub>)

The aged HC-F sample presented an important delamination of about 200  $\mu\text{m}$  thick at the edge. This oxidised path and delamination is also present inside

the sample with a similar thickness (figure 13 and zoom in figure 14). This delamination is not only the result of the aging. Indeed, it occurred on a peculiar sheet which separated two zones of different aspects already present on the reference sample.



Figure 13: Scan of an aged HC-F sample (4250 h, 155°C, 2.3 bar O<sub>2</sub>)

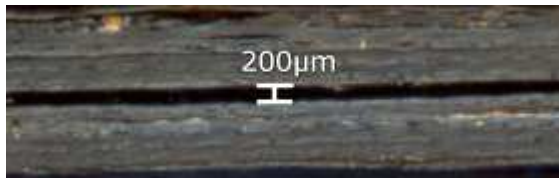


Figure 14: Zoom of the aged HC-F sample (4250 h, 155°C, 2.3 bar O<sub>2</sub>)

For the aged Class-H sample (figure 15 and zoom in figure 16), and contrary to the aged Ref-F sample, the edges present many voids, voids that doesn't go deep inside the sample. The largest voids are about 100 µm thick. Nevertheless, some local defects are also present inside the sample.



Figure 15 : Scan of an aged Class-H sample (740 h, 180°C, 2.3 bar O<sub>2</sub>)

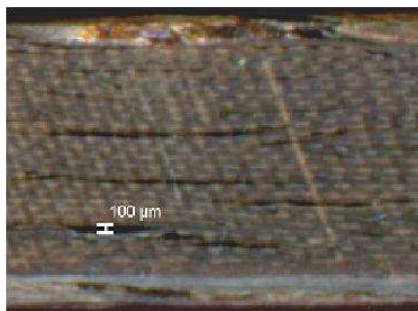


Figure 16: Zoom of the aged Class-H sample (740 h, 180°C, 2.3 bar O<sub>2</sub>)

## DISCUSSION

### Aged HC-F sample

The aged HC-F sample presented an important delamination of about 200 µm thick going through the

entire sample. With basic dielectric equations it is possible to estimate the electrical field ( $E_{air}$ ) in a cavity as shown in figure 17, where the width is much larger than the thickness (equation 1).



Figure 17: Simplified representation of a cavity in a sample

$$(1) \quad E_{air} = \frac{V}{x_{air} + \frac{\epsilon_{air}}{\epsilon_d}(d - x_{air})}$$

Equation 1 applied to the case of the aged HC-F sample, and with:

$$V = 3.8 \text{ kV}_{\text{rms}} \text{ (PDIV)}$$

$$d = 2 \text{ mm}$$

$$x_{air} = 200 \text{ } \mu\text{m} \text{ (delamination)}$$

$$\epsilon_{air} = 1$$

$$\epsilon_d = 3.4 \text{ (measured)}$$

Then :

$$E_{air} = 5.2 \text{ kV}_{\text{rms}} \cdot \text{mm}^{-1}$$

For an air film of 200 µm, at a pressure of 1 atm, the Paschen law [7-8] shows that the breakdown strength is about 5 kV<sub>rms</sub>·mm<sup>-1</sup>. For this sample, the estimated electrical field in the delamination using equation 1 is rather in good agreement with the calculated electrical field, using the Paschen law.

From this example, where the delamination of 200 µm is present through the entire sample, it seems possible to evaluate the thickness of the largest voids in an aged samples thanks to a PDIV measurement.

### Ref-F samples

For the new Ref-F sample, many PDs are present from PDIV on (figure 7). Nevertheless, the triangular shape of the positive half-period and the asymmetry between the two half-periods suggests that those PDs aren't coming from the sample but probably from a bubble trapped between the sample and the electrode. So, for this sample, it was not possible to estimate the maximum void size by the mean of the PDIV measurement.

For the aged Ref-F sample, only one “rabbit ear” can be seen on this pattern (figure 8). That seems to mean that there is a predominant single void in the sample. This is confirmed by the visual inspection of the sample, as only one delamination of 60 µm thick has been observed at the edge of the sample, delamination that goes deep inside the sample (figure 11). Using equation 1 and the Paschen law, the calculation leads to

a void size of 80  $\mu\text{m}$  thick, larger but of the same order of magnitude than the observed void size.

### Aged Class-H sample

For the aged Class-H sample the calculation gives a void size smaller (60  $\mu\text{m}$ ) than the largest void size observed (100  $\mu\text{m}$ ) at the edges of the sample. This is not surprising since, contrary to the aged Ref-F sample, the voids at the edges don't go deep inside the sample (figure 15). Nevertheless, some local defects are also present inside the sample which may explain this PDIV.

### Summary

We saw that the PDIV (or PD inception field for the HC-F) decreased during the samples aging. This is explained by the fact that, when the resin is aging, voids are appearing and are becoming larger and larger due to the thermo-oxidation. Table 2 summarizes the main results for the different samples: void sizes calculated using the Paschen law and the maximum void sizes observed at the edges of the samples.

Sample (aging time)	Void size calculated ( $\mu\text{m}$ )	Void size observed ( $\mu\text{m}$ )
Ref-F (805 h)	80	60
HC-F (new)	10	/
HC-F (4250 h)	200	200
Class-H (new)	35	/
Class-H (740 h)	60	100

Table 2: Calculated and observed void sizes

One can see that the sizes of the largest voids calculated with the PDIV and the Paschen law are rather in good agreement with the sizes of the largest voids observed at the edges or inside the samples.

### CONCLUSION

Three materials for the insulation of high voltage rotating machines have been submitted to an artificial thermo-oxidative aging and characterized using PD measurements.

Voids of a few tens of  $\mu\text{m}$  and macroscopic delaminations resulting from aging have been observed and quantified.

Partial Discharges measurement is a sensitive indicator of the size of the cavities resulting from aging. As a matter of fact, the measured Partial Discharge Inception Voltage (PDIV) revealed in good agreement with the theoretical voltage strength deduced from the Paschen law taken into account the thickness of the voids observed in the samples. Since PDs are issued from local defects, the comparison of materials on the basis of the absolute value of PDIV is not reasonable. However, material comparisons can be made on the

basis of the relative evolution of PDIV and the observation of delaminations on aged samples.

### REFERENCES

1. Ciutacu, S, Budrugaec, P, Nicolae, I, "Accelerated thermal aging of glass-reinforced epoxy resin under oxygen pressure", *Polymer Degradation And Stability*, 31, 365-372 (1991).
2. Tsotsis, T.K, Keller, S, Lee, K, Bardis, J, Bish, J, "Aging of polymeric composite specimens for 5000 hours at elevated pressure and temperature", *Composites Science and Technology*, 61, 75-86 (2001).
3. Boucher, V, Rain, P, Teissèdre, G, Schlupp, P, "Mechanical and Dielectric Properties of Glass-Mica-Epoxy Composites along Accelerated Thermo-Oxidative Aging", *IEEE - International Conference on Solid Dielectrics*, 162-165 (2007).
4. Boucher, V, Rain, P, Teissèdre, G, Schlupp, P, "Evolution of Structural Properties of Glass-Mica-Epoxy Insulation along Accelerated Thermo-Oxidative Aging", *IEEE - Conference on Electrical Insulation and Dielectric Phenomena*, 83-86 (2008).
5. Hudon, C, Bélec, M, "Partial Discharge Signal Interpretation for Generator Diagnostics", *IEEE Transaction on Dielectrics and Electrical Insulation*, 12, n°2, 297-319 (2005).
6. Contin, A, Cavallini, A, Montanari, G.C, Pasini, G, Puletti, F, "Digital Detection and Fuzzy Classification of Partial Discharge Signals", *IEEE Transaction on Dielectrics and Electrical Insulation*, 9, n°3, 335-348 (2002).
7. Kreuger, F.H, "Partial Discharge Detection in High-Voltage Equipment", Publ. By Butterworth & Co (1989).
8. Dakin, T.W, Luxa, G, Opperman, G, Vigreux, J, Wind, G, Winkel, H, "Phénomènes disruptifs dans un gaz en champ uniforme. Courbe de Paschen pour l'azote, l'air et l'hexafluorure de soufre", *Electra*, 32, 62-82 (1974).